Reductive Electron Transfer Quenching of MLCT Excited States Bound To Nanostructured Metal Oxide Thin Films

Bryan V. Bergeron and Gerald J. Meyer*

Department of Chemistry and Department of Materials Science and Engineering, Johns Hopkins University, 3400 North Charles Street, Baltimore, Maryland 21218

Received: August 23, 2002; In Final Form: October 28, 2002

The ruthenium compounds Ru(deeb)(bpz)$_2$(PF$_6$)$_2$, Ru(deeb)$_2$(bpz)(PF$_6$)$_2$, and Ru(deeb)$_2$(dpp)(PF$_6$)$_2$, where deeb is 4,4′-(CO$_2$CH$_2$CH$_3$)$_2$-2,2′-bipyridine, bpz is 2,2′-bipyrazine, and dpp is 2,3-bis(2-pyridyl)pyrazine, have been prepared, characterized, and anchored to mesoporous nanoparticle thin films comprised of the wide band gap semiconductor TiO_2 or the insulator ZrO_2. The metal-to-ligand charge-transfer (MLCT) excited states of these compounds are potent photooxidants ($E°(Ru^{II*/+}) > +1.0$ V vs SCE) with long lifetimes ($\tau > 1$ μs) that efficiently oxidize iodide and phenothiazine with rate constants that approach the diffusion limit in acetonitrile. Photogalvanic cells based on the sensitized TiO_2 materials yield photocurrent action spectra that agree well with the Ru(II) absorptance spectra. The photocurrent efficiency was very low, $\phi < 10^{-4}$. Transient absorption data show that neither the excited nor the reduced state of the ruthenium compounds efficiently inject electrons into the TiO_2 particles. The cage escape yields following excited-state electron transfer are approximately 2/3 lower in the mesoporous thin films than in fluid solution. Intermolecular energy transfer across the nanoparticle surfaces is manifest in a second-order component to the excited-state relaxation kinetics.

Introduction

Sensitization of semiconductor electrodes to visible light with molecular compounds represents an attractive approach to solar energy conversion.[1−3] In photoelectrochemical cells, selective light excitation of molecular chromophores, termed sensitizers, S, proximate to n-type semiconductor surfaces often yields anodic photocurrents. Two different interfacial electron-transfer mechanisms have been identified by which this photocurrent can be generated and sustained, Scheme 1. In one, termed excited-state dye sensitization, a photoexcited sensitizer, S*, injects an electron into the semiconductor, SC, and the sensitizer ground state is then regenerated by an electron donor, D, eq 1.

$$SC/S^* + D \xrightarrow{1.} SC(e^-)/S^+ + D \xrightarrow{2.} SC(e^-)/S + D^+ \quad (1)$$

In the other mechanism, a donor present in the electrolyte reductively quenches the excited sensitizer and the reduced state, S^-, transfers an electron into the semiconductor, eq 2. Solar cells based on this mechanism are often referred to as photogalvanic cells.[3]

$$SC/S^* + D \xrightarrow{1.} SC/S^- + D^+ \xrightarrow{2.} SC(e^-)/S + D^+ \quad (2)$$

In both mechanisms, [SC(e^-), D^+] charge-separated pairs are formed and the thermodynamically downhill charge recombination process, eq 3, must be prevented to yield a high photocurrent.

$$SC(e^-)/S + D^+ \xrightarrow{3.} SC/S + D \quad (3)$$

In photoelectrosynthetic cells, SC(e^-) and D^+ undergo subsequent redox reactions that yield chemical products. For regenerative cells, D^+ is reduced at a dark counter electrode and electrical power is generated with no net chemistry.[1−3]

The vast majority of early dye sensitization studies were performed on planar electrodes and relied strictly on photoelectrochemical measurements from which it was not possible to unambiguously distinguish between these two mechanisms.[4] More recently, dye sensitization studies have focused on mesoporous thin films of nanocrystalline (anatase) TiO_2. These materials have an enormous surface area, a long effective path length, and a high photoconductivity that affords both spectroscopic and photoelectrochemical characterization that can firmly establish sensitization mechanisms.[5] The observation of ultrafast electron injection[6] coupled with the weak oxidizing power of the excited sensitizers currently in use,[7] strongly suggest an excited-state injection mechanism is operative in regenerative solar cells based on these materials.[5]

Strong spectroscopic evidence for the reduced sensitizer injection mechanism with sensitized mesoporous thin films was recently reported.[8] Interfacial electron transfer was shown to be rate-limited by reductive quenching of the sensitizer excited state, eq 2. The sensitizer used in this work was Ru(deeb)(bpy)$_2$(PF$_6$)$_2$, where deeb is 4,4′-(CO$_2$CH$_2$CH$_3$)$_2$-2,2′-bipyridine and bpy is 2,2′-bipyridine, and the electron donor was phenothiazine, PTZ. A drawback of the PTZ donors is that they produce negligible photocurrents in the dye-sensitized nanocrystalline solar cells.[9] Iodide is the sole electron donor identified that yields solar energy conversion efficiencies >10% under one sun of AM 1.5 solar irradiation.[10] Ru(deeb)(bpy)$_2^{2+*}$ and other Ru(II) bipyridyl excited states are weak photooxidants that do not efficiently oxidize iodide.[8]

In this work we have prepared new Ru(II) sensitizers, with functional groups for surface attachment, that are potent excited-state oxidants capable of efficient iodide oxidation. We present photophysical and reductive electron-transfer studies of these compounds in fluid acetonitrile and when bound to colloidal

* Corresponding author.

10.1021/jp026823n CCC: $25.00
Published on Web 12/03/2002

SCHEME 1

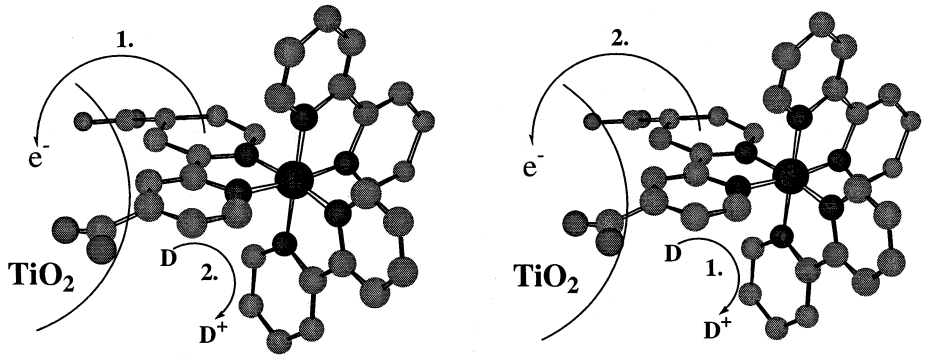

Excited State Dye Sensitization **Reduced State Dye Sensitization**

TiO_2 and ZrO_2 mesoporous thin films. Unlike previous studies, we find examples where neither the sensitizer's reduced state nor excited-state transfers electrons to the semiconductor efficiently.[8] The results demonstrate a general approach for photogenerating oxidizing and reducing equivalents with well-defined molecular structures that store >2 eV of free energy.

Experimental Section

Materials. $RuCl_3.xH_2O$ (~ 42% Ru) was used as received from Johnson Matthey. The following materials were obtained from Aldrich and used as received: $CuSO_4 \cdot 5H_2O$ (98%), 2-pyrazinecarboxylic acid (99%), hydroquinone (99%), 4,4′-dimethyl-2,2′-dipyridyl (99%), LiCl (99%), ammonium hexafluorophosphate (95%), tetrabutylammonium hexafluorophosphate, TBAH (98%), tetrabutylammonium iodide (98%), tetraethylammonium chloride hydrate (98%), $LiClO_4$ (95%), 2,3-bis(2-pyridyl)pyrazine (98%), CH_3CN, DMSO, $CDCl_3$, and DMSO-d_6. Phenothiazine (Aldrich, 98%) was recrystallized from toluene prior to use. $Ru(deeb)_2(Cl)_2$, $Ru(deeb)(bpy)_2(PF_6)_2$, and 2,2′-bipyrazine (bpz) were prepared as previously described.[11−13]

Preparations. *Ru(deeb)$_2$(dpp)(PF$_6$)$_2$.* $Ru(deeb)_2Cl_2$ (535 mg, 0.693 mmol) and a 4-fold excess of 2,3-bis(2-pyridyl)pyrazine (310 mg, 1.32 mmol) were combined in 115 mL of ethanol/water (50:50) and the mixture was refluxed for 8−10 h. The orange/red solution was allowed to cool to room temperature and filtered to remove unreacted ligand. Approximately 40 mL of a 0.2 M $KPF_{6(aq)}$ was combined with the solution and an immediate orange precipitate formed that was filtered and dried under vacuum (76%). Mass spectrum, $(M + 1)^+ = 1082$ (calcd. 1082), $(M + 1)^{2+} = 937$ (calcd. 937). Anal. Calcd. for $C_{46}N_8O_8H_{42}P_2F_{12}Ru$: C, 45.06; N, 9.14; H, 3.45. Found: C, 44.39; N, 9.19; H, 3.47. ^{1}H NMR ($(CD_3)_2SO$) δ: 1.35 (t, 6H, CH_3), 1.37 (t, 6H, CH_3), 4.42 (q, 4H, CH_2), 4.46 (t, 4H, CH_2), 7.16 (d, 1H, $J = 7.9$ Hz), 7.32−7.45 (m, 1H), 7.69−8.27 (m, 14H), 8.66−8.70 (m, 2H), 9.36 (s, broad, 4H).

Ru(deeb)$_2$(bpz)(PF$_6$)$_2$. $Ru(deeb)_2Cl_2$ (384 mg, 0.497 mmol) and 2,2′-bipyrazine (315 mg, 1.99 mmol) were combined in 100 mL of ethanol/water (50:50) and refluxed for 3 days. The orange/red solution was allowed to cool to room temperature and filtered to remove unreacted ligand. Upon addition to 15 mL of 0.2 M $KPF_{6(aq)}$ an immediate orange/red precipitate formed that was filtered and dried under vacuum (56%). Mass spectrum, $M^+ = 1005$ (calcd. 1005), $M^{2+} = 860$ (calcd. 860). Calcd. for $C_{40}N_8O_8H_{38}P_2F_{12}Ru$: C, 41.78; N, 9.75; H, 3.33. Found: C, 41.24; N, 9.69; H, 3.41. ^{1}H NMR ($(CD_3)_2SO$) δ: 1.35 (t, 6H, CH_3), 1.36 (t, 6H, CH_3), 4.44 (q, 4H, CH_2), 4.45 (q, 4H, CH_2), 7.85 (d, 4H, $J = 5.9$ Hz), 7.92 (d, 2H, $J = 5.9$ Hz), 7.96 (d, 2H, $J = 2.6$ Hz), 8.03 (d, 2H, $J = 6.1$ Hz), 8.67 (s, 2H, $J = 2.6$ Hz), 9.34 (s, 4H), 10.14 (s, 2H).

Ru(Me$_2$SO)$_4$(Cl)$_2$. $Ru(Cl)_3 \cdot xH_2O$ (660 mg, 2.74 mmol Ru) was refluxed in 20 mL of DMSO under argon. The solution first turned red within 1−2 h, then yellow. After the solution cooled to room temperature, addition of 20 mL of acetone yielded a yellow precipitate that was filtered and rinsed with ether (302 mg, 23%).

Ru(bpz)$_3$(PF$_6$)$_2$. $Ru(Me_2SO)_4(Cl)_2$ (400 mg, 1.1 mmol) and bpz (800 mg, 5.06 mmol) were refluxed in 30 mL of H_2O for 20 h. The reaction mixture was allowed to cool to room temperature and filtered. The solution was combined with 10 mL of 2 mM $KPF_{6(aq)}$, resulting in the formation of an orange precipitate. The filtered crude product was rinsed with 5 mL of water and recrystallized in 70 mL of acetone/ethanol 6:1 (151 mg, 28%). ^{1}H NMR ($(CD_3)_2SO$) δ: 8.00 (d, 6H, $J = 3.2$ Hz), 8.71 (d, 6H, $J = 3.2$ Hz), 10.14 (s, 6H).

Ru(bpz)$_2$(Cl)$_2$. A solution of $Ru(bpz)_3(PF_6)_2$ (150 mg, 0.174 mmol) and tetraethylammonium chloride hydrate, $TEACl \cdot H_2O$, (2.5 g, 15 mM) were combined in 750 mL of argon-saturated CH_3CN and stirred. The mixture was irradiated using a 1000 W Xe lamp with a UV cutoff prefilter. Absorbance readings were taken periodically to monitor the extent of the reaction over approximately 12 h. The deep purple solution was filtered and the solvent volume was reduced to approximately 60 mL and this caused precipitation of the desired product, $Ru(bpz)_2(Cl)_2$. Filtration, followed by washing with acetonitrile, gave purple crystals (30 mg, 35%).

Ru(deeb)(bpz)$_2$(PF$_6$)$_2$. $Ru(bpz)_2(Cl)_2$ (40 mg, 0.0826 mmol) and 4,4′-$(CO_2CH_2CH_3)_2$-2,2′-bipyridine (74 mg, 0.247 mmol) were combined in 8 mL of ethanol/water (50:50) and the mixture was refluxed for 8 h. The solution was allowed to cool to room temperature and filtered. Approximately 10 mL of 0.1 M $KPF_{6(aq)}$ was combined with the solution resulting in formation of a precipitate that was isolated by filtration (43 mg, 52%). Anal. Calcd. for $C_{32}N_{10}O_4H_{28}P_2F_{12}Ru$: C, 38.14; N, 13.90; H, 2.80. Found: C, 36.94; N, 13.80; H, 2.88. ^{1}H NMR ($(CD_3)_2SO$) δ: 1.36 (t, 6H, CH_3), 4.45 (q, 4H, CH_2), 7.86 (dd, 2H, $J = 5.9$ Hz, $J = 2.2$ Hz), 7.90 (d, 2H, $J = 2.2$ Hz), 8.00 (d, 2H, $J = 5.9$ Hz), 8.05 (d, 2H, $J = 3.3$ Hz), 8.67 (d, 2H, $J = 3.2$ Hz), 8.72 (d, 2H, $J = 2.2$ Hz), 9.34 (d, 2H, $J = 2.2$ Hz), 10.13 (s, 2H), 10.14 (s, 2H).

Colloidal MO_2 Films. Colloidal TiO_2 and ZrO_2 films were prepared as previously described.[13] The metal oxide films were placed in a pH 11 aqueous solution (NaOH) for 1 h, rinsed in neat acetonitrile, and were then exposed to mM concentrations of the Ru(II) compounds for at least 12 h. The films were rinsed

in neat acetonitrile before spectroscopic, electrochemical, or photoelectrochemical measurements.

Measurements. *Absorption.* All absorption measurements were acquired by placing the TiO_2 or ZrO_2 on glass films diagonally in an acetonitrile filled 10 mm × 10 mm quartz cuvette, equipped with a 24/40 ground quartz joint. The cell was closed with a PTFE stopper and purged with argon through a glass capillary tube, when indicated. Ground-state absorption spectra were acquired at ambient temperature in air using a Hewlett-Packard 8453 diode array spectrophotometer.

Transient absorption spectra were acquired as previously described. Briefly, an approximately 7 ns, 532 nm laser pulse from a Surelite II Nd:YAG, Q-switched laser was used as the excitation source. The approximately 1 cm beam was expanded using a quartz concave lens as a means of both course attenuation of the excitation energy and ensuring homogeneous irradiation of the sample.[13] The energy was often further attenuated using a polarizing prism of local design. Each kinetic trace was acquired by averaging 10−400 laser shots (typically 80) at a repetition rate of 1 Hz. Excitation was carried out such that the entire exposed TiO_2 surface of the sample, positioned at an approximately 45° angle to the excitation beam, was irradiated. The Xe probe (150 W, Applied Photophysics, operating in pulsed mode) was positioned normal to the excitation beam.

Photoluminescence. Steady-state photoluminescence (PL) spectra were obtained with a Spex Fluorolog that had been calibrated with a standard NIST tungsten−halogen lamp. Time-resolved photoluminescence (TRPL) decays were acquired with an apparatus that has been previously described.[14]

Steady-State Photoreductions. The ruthenium compounds were excited with ∼120 mW/cm^2 of 514.5 nm light (Coherent Innova 70 Argon Ion Laser) in a 0.3 M triethylamine, argon-purged acetonitrile solution. These photoreductions were performed in the cuvette holder of an HP 8453 diode array spectrophotometer and the changes in absorption as a function of irradiance were monitored.

Electrochemistry. All cyclic voltammograms were recorded on a BAS 50 electrochemical analyzer in 0.1 M TBAH acetonitrile solution. A Ag/AgCl reference electrode with Pt gauze auxiliary and Pt working electrode comprised the three electrode cell. All samples were extensively purged with argon, and the reference occasional monitored for a drift in potential using ferrocene as a standard.

Photoelectrochemistry. Photoelectrochemical measurements were made as previously described.[10a]

NMR. All ^{1}H NMR data was obtained on a Bruker AMX 300 Spectrometer.

Results

Figure 1 shows the room-temperature absorption and photoluminescence, PL, spectra of $Ru(deeb)_2(bpz)^{2+}$ in fluid solution, and when anchored to colloidal TiO_2 and ZrO_2 films and immersed in argon-saturated acetonitrile. The metal-to-ligand charge transfer (MLCT) bands broaden slightly and the PL maximum red shifts upon surface attachment. The optical properties of $Ru(deeb)(bpz)_2^{2+}$ and $Ru(deeb)_2(dpp)^{2+}$ in solution and when bound to the metal oxide surfaces are qualitatively similar, Table 1. Throughout the Results Section, typical data for $Ru(deeb)_2(bpz)^{2+}$ is shown; the corresponding data for $Ru(deeb)(bpz)_2^{2+}$ and $Ru(deeb)_2(dpp)^{2+}$ are given in the Supporting Information. The ligands are shown below for clarity.

Reversible reductions of the Ru(II) compounds were observed by cyclic voltammetry in 0.1 M TBAH acetonitrile electrolyte

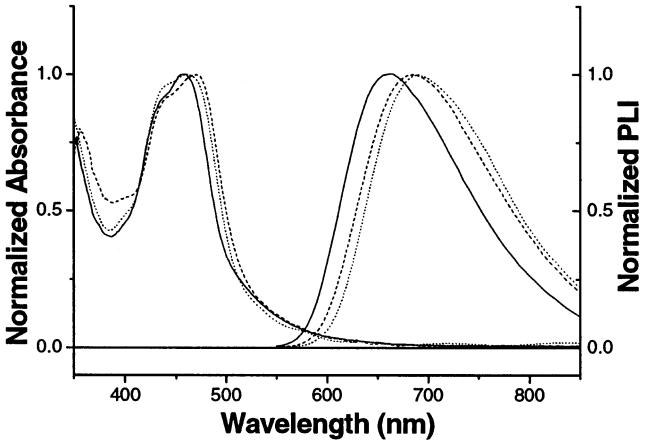

Figure 1. Normalized absorbance and steady-state photoluminescence of $Ru(deeb)_2(bpz)(PF_6)_2$ in acetonitrile (—), on TiO_2 (− −), and on ZrO_2 (- - -).

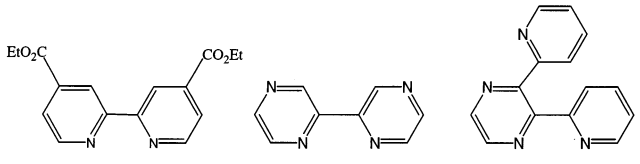

solution. The measured reduction potentials, and the free energy stored in the excited state, ΔG_{es}, were used to estimate the excited-state reduction potentials with eqs 4 and 5, Table 2.

$$E°(Ru^{II*/+}) = E°(Ru^{II/+}) + \Delta G_{es} \quad (4)$$

$$E°(Ru^{III/II*}) = E°(Ru^{III/II}) - \Delta G_{es} \quad (5)$$

The energy stored in the thermally equilibrated excited state, ΔG_{es}, was estimated with a tangent line extrapolated to zero intensity on the high-energy side of the corrected PL spectra.[15] We were unable to measure sensitizer reduction potentials when the sensitizer was anchored to the metal oxide surface. In previous work, we have found that the solution and surface-bound Ru(III/II) potentials are within ±20 mV the same.[13] There is a measurable shift in the photoluminescence spectra of the surface-bound compounds relative to solution values. Therefore, in estimating the reducing and oxidizing power of the surface-bound sensitizers, solution potentials and surface photoluminescence data were used in conjunction with eqs 4 and 5. The first oxidation of PTZ was found to be reversible with $E°(PTZ^{+/0}) = 0.58$ V vs SCE.

Time-resolved PL decays of $Ru(deeb)_2(bpz)^{2+*}$ and the other Ru(II)* compounds in solution were fit to a first-order kinetic model given in eq 6. The TRPL of Ru(II)* compounds bound to TiO_2 and ZrO_2 were nonexponential and were well described by a parallel first- and second-order kinetic model, eqs 7 and 8,

$$I(t) = A(\exp(-k_1 t)) \quad (6)$$

$$I(t) = C(k_1 \exp(-k_1 t))/(k_1 + p - p(\exp(-k_1 t))) \quad (7)$$

$$p = k_2[Ru^{2+*}]_{t=0} \quad (8)$$

where C is a constant, and k_1 and k_2 are the first- and second-order rate constants, respectively.[16]

TABLE 1: Photophysical Properties of Ru(II) Sensitizers on MO_2 and in Acetonitrile[a]

sensitizer[b]	$\lambda_{abs.}$(nm)[c]	λ_{PL} (nm)[d]	ϵ (M^{-1} cm^{-1})	τ (μs)[e]
$Ru(deeb)(bpy)_2^{2+}$(sol)	475	690	16000	0.990
$Ru(deeb)(bpy)_2^{2+}(TiO_2)$	457	656		1.04
$Ru(deeb)(bpy)_2^{2+}(ZrO_2)$	461	671		1.30
$Ru(deeb)_2(dpp)^{2+}$(sol)	464	643	21200 ± 400	1.48
$Ru(deeb)_2(dpp)^{2+}(TiO_2)$	464	670		0.90
$Ru(deeb)_2(dpp)^{2+}(ZrO_2)$	464	675		0.67
$Ru(deeb)_2(bpz)^{2+}$(sol)	458	658	18100 ± 600	1.31
$Ru(deeb)_2(bpz)^{2+}(TiO_2)$	436−472[f]	683		0.56
$Ru(deeb)_2(bpz)^{2+}(ZrO_2)$	466	683		0.63
$Ru(deeb)(bpz)_2^{2+}$(sol)	449	636	14460 ± 200	1.78
$Ru(deeb)(bpz)_2^{2+}(TiO_2)$	458	668		0.94
$Ru(deeb)(bpz)_2^{2+}(ZrO_2)$	457	681		1.14

[a] All measurements made at room temperature. [b] The Ru(II) sensitizers with ligand abbreviations defined in the text. The measurements were made in fluid acetonitrile (sol), and attached to (TiO_2) and (ZrO_2) thin films immersed in an acetonitrile bath. [c] The visible MLCT absorption maximum. [d] The photoluminescence maximum, ±8 nm. [e] Excited-state lifetime, ± 5%. Excited-state relaxation on TiO_2 and ZrO_2 was found to be nonexponential. The first-order component abstracted from a parallel first- and second-order kinetic model were used to estimate the lifetime. See text for details. [f] A broad absorption band with no clear maximum.

TABLE 2: Ground- and Excited-State Sensitizer Reduction Potentials[a]

sensitizer	$E°(Ru^{III/II})$	$E°(Ru^{II/+})$	$E°(Ru^{III/II*})$	$E°(Ru^{II*/+})$
$Ru(deeb)(bpy)_2^{2+}$	1.39	−1.0	−0.62	1.01
$Ru(deeb)_2(dpp)^{2+}$	1.59	−0.92	−0.57	1.24
$Ru(deeb)_2(bpz)^{2+}$	1.73	−0.82	−0.38	1.31
$Ru(deeb)(bpz)_2^{2+}$ [b]		−0.82		1.36

[a] Potentials measured versus SCE in 0.1 M TBAH acetonitrile electrolyte at room temperature. The ground-state potentials were measured by cyclic voltammetry and the excited-state potentials were estimated with eqs 4 and 5. [b] The reduction potentials of this compound were not measured. The first reduction is expected to be bpz-based so the $E°(Ru^{II/+})$ of $Ru(deeb)_2(bpz)^{2+}$ was assumed.

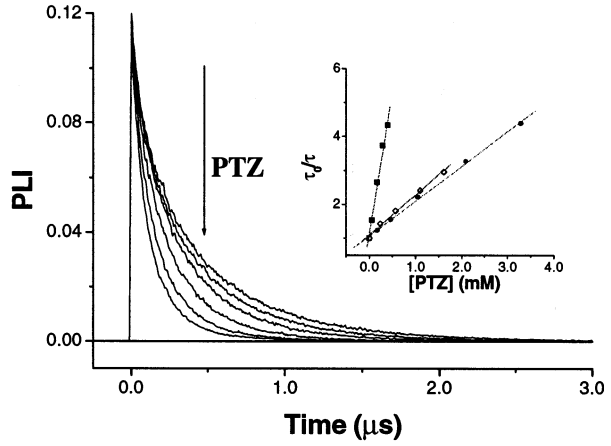

Figure 2. Time-resolved photoluminescence quenching of $Ru(deeb)_2(bpz)(PF_6)_2$ bound to TiO_2 with PTZ following 460 nm excitation. Inset shows a Stern−Volmer analysis for solution (■), bound to TiO_2 (●), and bound to ZrO_2 (◇).

The introduction of phenothiazine into the acetonitrile solution resulted in excited-state quenching at homogeneous and heterogeneous environments. Figure 2 displays time-resolved PL decays after pulsed light excitation of $Ru(deeb)_2(bpz)^{2+}$ in argon-saturated acetonitrile with increasing concentrations of phenothiazine, PTZ. Dynamic quenching was apparent for both solution and surface experiments with no evidence for static processes.[17] Stern−Volmer analysis was used to quantify the quenching dynamics, eq 9, Figure 2 inset.

$$\tau_o/\tau = 1 + K_{sv}[Q] \tag{9}$$

In eq 9, the Stern−Volmer constant, K_{sv}, is equal to $k_q\tau_o$ where τ_o is the lifetime in the absence of PTZ.[17] For the surface-bound sensitizers, lifetimes were determined by fixing p in eqs 7 and 8 to the value determined in the absence of PTZ, and allowing k_1 to float until the best fit was obtained, with $\tau = 1/k_1$. Excellent fits via this method were obtained for both solution and surface quenching. Table 3 summarizes these results for $Ru(deeb)_2(bpz)^{2+}$ and the other compounds. Quenching studies with iodide were also performed and reveal rapid and efficient iodide oxidation, $k_q > 10^8$ M^{-1} s^{-1}. The transient absorption details with iodide are more complex and will be the focus of a separate paper.[18]

Figure 3 shows transient absorption difference spectra recorded after pulsed 532 nm light excitation of $Ru(deeb)_2(bpz)^{2+}$ in fluid solution and when bound to TiO_2 and ZrO_2 films immersed in argon-saturated acetonitrile. Within reasonable experimental error, the difference spectra are the same in all three cases and are typical of MLCT excited states with positive absorption bands at ~ 380 nm, a bleach at ~ 450 nm, and an isosbestic point at 398 nm.[16] In fluid acetonitrile, the kinetics were first-order and when anchored to TiO_2 and ZrO_2 they were well-described by the parallel first- and second-order kinetic model with rate constants that agreed well with those obtained by TRPL measurements.

Transient absorption difference spectra recorded after pulsed 532 nm light excitation of $Ru(deeb)_2(bpz)^{2+}$ in argon-saturated acetonitrile solution in the presence of PTZ are shown in Figure 4. The MLCT excited state was observed initially that evolved into a new state with positive absorption bands at 380 and 520 nm, assigned to a $[Ru(II)(L^-)^+/PTZ^+]$ charge-separated state. Within experimental error, the rate constants for appearance of the charge-separated state agree with those measured by dynamic PL quenching. At high PTZ concentrations, it was difficult to transmit light below 400 nm due to competitive light absorption by the PTZ. Therefore, the data shown was collected at 3−4 mM PTZ which corresponds to nearly complete quenching of the Ru(II) excited states in solution and ~75% within the mesoporous thin films. Normalized absorption difference spectra obtained at >5 μs after the laser pulse are within experimental error the same on ZrO_2 and TiO_2 materials.

On a much longer time scale than is shown, the charge-separated state decays to ground-state products. Figure 5 shows transient absorption kinetics that correspond to electron transfer from the reduced ruthenium compound to PTZ^+ both in solution and anchored to TiO_2. The PTZ concentrations were kept high to ensure that >99% of the excited states were quenched. Figure 5 shows that the yield of charge-separated pairs is about 3 times larger in fluid solution. About 1/2 of the charge-separated states formed in the mesoporous film recombine in the first microsecond while there is negligible recombination in fluid solution on this same time scale. UV−Vis absorption measurements before and after the time-resolved studies revealed no evidence for permanent photochemistry.

Chemical and photochemical redox reactions were performed to obtain the visible absorption spectra of the oxidized phenothiazine, PTZ^+, and the reduced ruthenium compounds. The stoichiometric addition of bromine to a PTZ acetonitrile solution leads to the appearance of the PTZ^+ absorption spectrum. Photochemical reductions of the Ru(II) compounds were obtained with 514.5 nm light excitation in the presence of the

TABLE 3: Excited-State Reductive Electron Transfer Rate Constants[a]

sensitizer	K_{sv}[b] (M^{-1})	k_q[b] ($10^{-9}\,M^{-1}\,s^{-1}$)	k_e[c] ($10^{-9}\,M^{-1}\,s^{-1}$)	$-\Delta G$[d] (eV)
$Ru(deeb)(bpy)_2^{2+}$(sol)	6030 ± 300	6.09 ± 0.30	8.58 ± 0.43	0.43
$Ru(deeb)(bpy)_2^{2+}(TiO_2)$	1190 ± 50	1.15 ± 0.06	1.22 ± 0.06	0.56
$Ru(deeb)(bpy)_2^{2+}(ZrO_2)$	1200 ± 60	1.53 ± 0.08	1.65 ± 0.08	0.53
$Ru(deeb)_2(dpp)^{2+}$(sol)	10200 ± 500	6.89 ± 0.34	10.3 ± 0.51	0.61
$Ru(deeb)_2(dpp)^{2+}(TiO_2)$	1130 ± 60	1.25 ± 0.06	1.33 ± 0.07	0.58
$Ru(deeb)_2(dpp)^{2+}(ZrO_2)$	1080 ± 50	1.61 ± 0.08	1.74 ± 0.09	0.60
$Ru(deeb)_2(bpz)^{2+}$(sol)	9900 ± 500	7.57 ± 0.38	11.8 ± 0.59	0.73
$Ru(deeb)_2(bpz)^{2+}(TiO_2)$	1010 ± 50	1.79 ± 0.09	1.96 ± 0.10	0.68
$Ru(deeb)_2(bpz)^{2+}(ZrO_2)$	1101 ± 55	1.75 ± 0.09	1.91 ± 0.10	0.77
$Ru(deeb)(bpz)_2^{2+}$(sol)	13900 ± 700	7.79 ± 0.39	12.4 ± 0.62	0.78
$Ru(deeb)(bpz)_2^{2+}(TiO_2)$	2080 ± 100	2.22 ± 0.11	2.48 ± 0.12	0.71
$Ru(deeb)(bpz)_2^{2+}(ZrO_2)$	2380 ± 120	2.09 ± 0.10	2.32 ± 0.12	0.79

[a] All measurements were performed in 0.1 M TBAH acetonitrile electrolyte with the electron donor phenothiazine. [b] Stern−Volmer, K_{sv}, and observed quenching rate constants. [c] Electron-transfer rate constants calculated with eq 13. [d] Driving force for Ru(II)* reduction by phenothiazine.

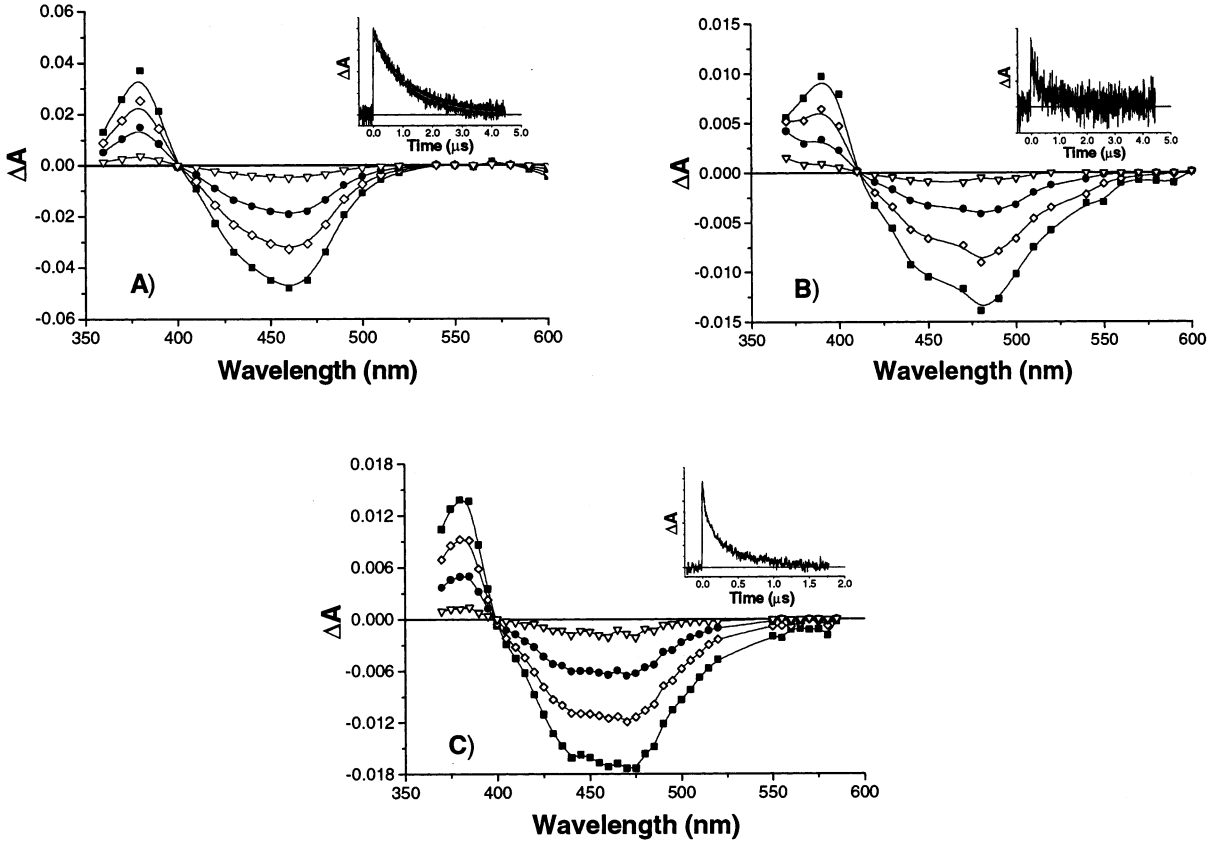

Figure 3. Transient absorption spectra of $Ru(deeb)_2(bpz)(PF_6)_2$ in 0.1 M TBAH acetonitrile electrolyte following 532 nm laser excitation (A) in acetonitrile at 0 ns (■), 500 ns (◇), 1200 ns (●), and 3000 ns (▽); (B) bound to TiO_2 at 0 ns (■), 80 ns (◇), 300 ns (●), and 1500 ns (▽); and (C) bound to ZrO_2 at 0 ns (■), 120 ns (◇), 300 ns (●), and 1000 ns (▽).

sacrificial donor triethylamine in argon saturated acetonitrile solutions. Typical data for the excited-state reduction of $Ru(deeb)_2(bpz)^{2+}$ anchored to colloidal TiO_2 and ZrO_2 are shown in Figure 6. The observed spectra were stable for short time periods and returned to yield ground-state spectrum on a minutes time scale. The absorption spectra of a 1:1 ratio of the reduced ruthenium compound to PTZ^+ were constructed and are superimposed on the data in Figure 4. The agreement between the simulated spectra and those observed transiently was good over the visible range. Below 400 nm, where the materials absorb strongly, the simulated spectra have a slightly lower amplitude.

The light-to-electrical energy conversion efficiency of these materials was measured in a two-electrode configuration with a Pt counter electrode and a 0.5 M tetrabutylammonium iodide/0.05 M I_2 acetonitrile electrolyte. The photocurrent action spectrum agrees well with the sensitizer absorptance spectrum. However, the photocurrent efficiency is very low, $\phi < 10^{-4}$ for all the sensitizers studied.

Discussion

A goal of this study was to prepare Ru(II) coordination compounds with long-lived strongly oxidizing, excited states that can be anchored to semiconductor surfaces for applications in dye-sensitized photogalvanic cells. The Ru(II) compounds synthesized with bipyrazine, bpz, or dipyridylpyrazine, dpp, ligands are potent photooxidants, $E°(Ru^{II*/+}) > +1.0$ V vs SCE, with microsecond excited-state lifetimes. The deeb ligands bind

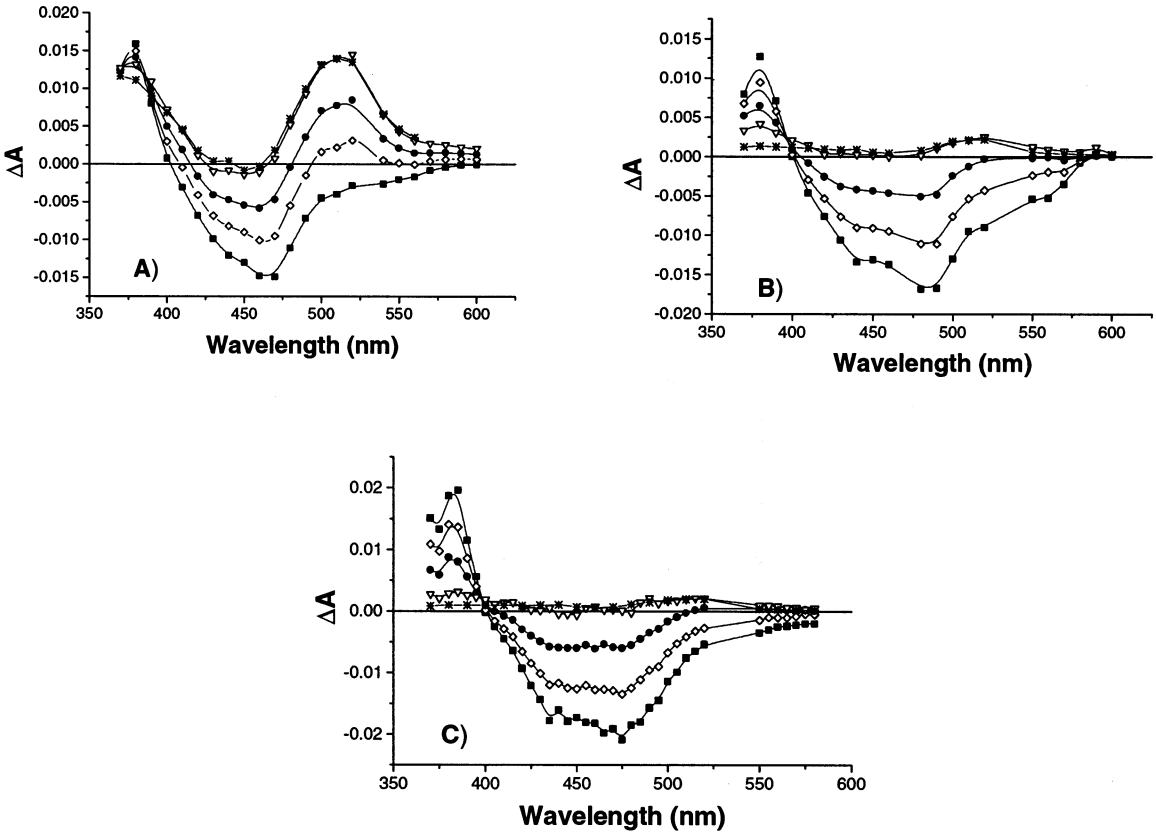

Figure 4. Transient absorption difference spectra of $Ru(deeb)_2(bpz)(PF_6)_2$ in 0.1 M TBAH acetonitrile electrolyte following 532 nm laser excitation (A) in acetonitrile with 3 mM PTZ at 0 ns (■), 20 ns (◇), 50 ns (●), and 300 ns (▽); (B) bound to TiO_2 with 3.5 mM PTZ at 0 ns (■), 15 ns (◇), 60 ns (●), and 1000 ns (▽); and (C) bound to ZrO_2 with 1.6 mM PTZ at 0 ns (■), 30 ns (◇), 120 ns (●), and 3000 ns (▽). Superimposed on the final difference spectra are simulated spectra (*).

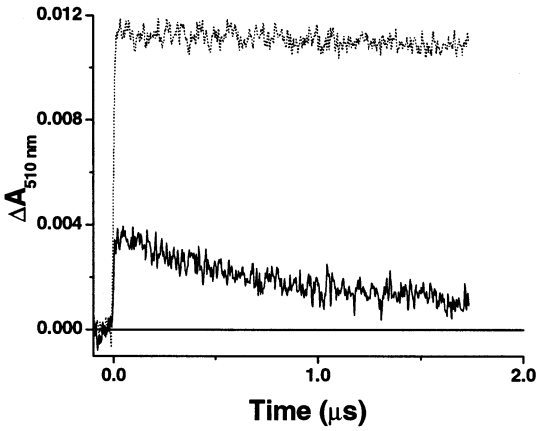

Figure 5. Absorption change monitored at 510 nm following pulsed 532.5 nm light excitation of $Ru(deeb)_2(bpz)(PF_6)_2$ in 0.1 M TBAH acetonitrile electrolyte in fluid electrolyte solution (upper trace) and when anchored to TiO_2 (lower trace).

tenaciously to metal oxide surfaces resulting in high surface coverages of the Ru(II) compounds on the semiconductor surface.[3] The light-to-electrical energy conversion efficiency of the materials in photogalvanic cells was, however, disappointingly low. Time-resolved spectroscopic measurements provide keen insights into the loss mechanisms and suggest methods for future optimization.

Below, we discuss the photophysical and electron-transfer studies of these molecular excited states. Since the metal-to-ligand charge-transfer (MLCT) excited states of Ru(II) compounds have been previously reported in the literature,[19,20] we restrict our discussion to the behavior on nanocrystalline (anatase) TiO_2 surfaces. The results identify important loss mechanisms relevant to solar energy conversion and also demonstrate an approach for photogenerating oxidizing and reducing equivalents with well-defined structures and potentials on semiconductor surfaces.

Excited States. The steady-state absorption and photoluminescence spectra of the Ru(II) compounds bound to the nanoparticle oxide surfaces are only slightly shifted from that observed in fluid solution, indicating that the compounds retain their coordination sphere upon surface binding and the emissive and absorptive states are largely unperturbed. The ethyl ester groups on deeb ligands are known to hydrolyze upon reaction with the TiO_2 surface.[3] For these sensitizers, the red-shifted photoluminescence spectra upon surface binding reflect decreased π back-bonding to the Ru center by the deeb ligands.

Time-resolved absorption difference spectra are those expected for the MLCT excited state and indicate negligible excited-state electron injection into the semiconductor, $\phi_{inj} < 0.05$. Injection from the thermally equilibrated excited state, vibrationally "hot" excited states, and the Franck−Condon excited state are not expected on consideration of the interfacial energetics. For example, 532.5 nm light excitation of $Ru(deeb)_2(bpz)^{2+}$ yields a Franck−Condon excited state with a reduction potential of −0.60 V vs SCE and vibrational relaxation to the thermally equilibrated state yields an even weaker photoreductant (Table 2). The energetic position of E_{cb} has been estimated to be −2.24 V vs SCE in 0.2 M $TBAClO_4/CH_3CN$.[30] Excited-state injection is consequently not expected on energetic grounds and is not observed. Therefore, these compounds provide an opportunity to study molecular excited states anchored to semiconductor surfaces without complications from interfacial

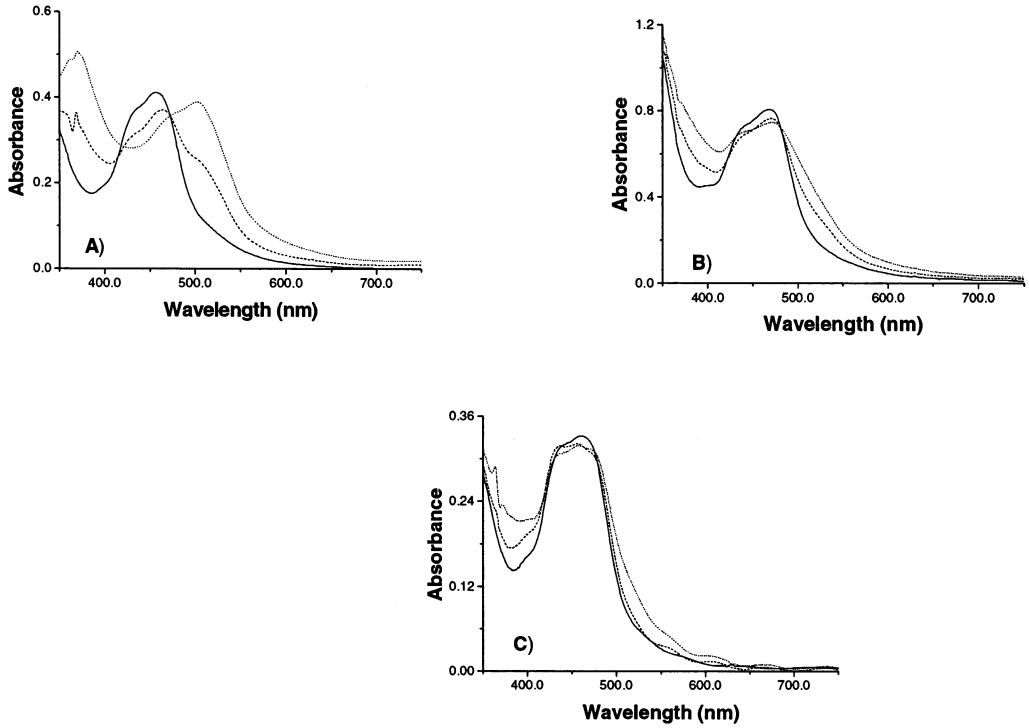

Figure 6. Steady-state photolysis of $Ru(deeb)_2(bpz)(PF_6)_2$ with 514 nm laser excitation in the presence of 0.3 M triethylamine with 0.1 M tetrabutylammonium hexafluorophosphate in argon-purged acetonitrile in (A) solution, (B) bound to TiO_2, and (C) bound to ZrO_2.

electron transfer. We note that the prediction of interfacial energetics for the operational solar cell (with I^-/I_3^-) is problematic as there exists no unambiguous method for determining E_{cb} under these conditions.

A notable difference between excited states in fluid solution and attached to metal oxide nanoparticles is the relaxation kinetics. In fluid solution, exponential kinetics are observed with a rate constant equal to the sum of a radiative and a nonradiative rate constant.[19] This behavior is expected for MLCT excited states.[19] In contrast, the excited states anchored to ZrO_2 or TiO_2 are nonexponential and are adequately described by a parallel first- and second-order kinetic model that has been previously derived.[16] The first-order rate constant corresponds to the "normal' solution relaxation pathways. The second-order component is attributed to a competitive bimolecular reaction, proposed to be a triplet−triplet annihilation reaction, rate-limited by energy transfer migration between the ground and excited states of adjacent, surface-attached molecules. In fluid solution, rate limitations imposed by the solvent are sufficient to prevent observation of such processes. However, these mesoporous nanocrystalline films have a high local concentration of the Ru(II) compounds, thought by many to be monolayer surface coverage.[2] Constraining these compounds in close proximity promotes intermolecular energy migration, and several examples on metal oxide nanoparticles are now documented in the literature.[16,21] Energy migration across the nanocrystalline semiconductor surface provides a mechanism for two excited states to encounter and react with each other. The reaction is reported to be a triplet−triplet annihilation process and proceeds with a rate constant greater than 10^8 s^{-1}.[22] The products are unknown in the present work, but have been the subject of much discussion in the MLCT literature.[22]

Excited-state annihilation reactions are unwanted and can lower the efficiency of solar energy conversion schemes based on diffusional quenching. It is therefore of interest to identify conditions that minimize the bimolecular excited-states decay pathway. Remarkably, we have been unable to find literature protocols for directly quantifying the fraction of excited states that decay through a given pathway. Qualitatively, we have observed that low sensitizer surface coverages and irradiances favor the first-order relaxation while the second-order pathway is predominant at high surface coverages and irradiances.[16] However, low surface coverages result in less sunlight being harvested and this is undesirable for solar conversion applications. At the lowest irradiances used, ~ 1 mW/cm^2, and the optimal maximum surface coverages, a second-order component was clearly present. A standard for solar cell testing is one sun of air mass 1.5 solar irradiation that corresponds to a steady-state irradiance of 100 mW/cm^2. This suggests that excited-state annihilation processes are a factor that would lower the efficiency of photogalvanic cells based on this approach.

Photoinduced Electron Transfer. Electron transfer from phenothiazine, PTZ, efficiently quenches the MLCT excited-states donors, eq 10. Time-resolved and spectroelectrochemical absorption

$$Ru(deeb)_2(bpz)^{2+}* + PTZ \xrightarrow{k_q} Ru(deeb)_2(bpz^-)^+ + PTZ^+ \quad (10)$$

measurements clearly demonstrate that PTZ^+ and the reduced ruthenium compound are present following photoexcitation in the expected 1:1 stoichiometry. Approximately 2.2 eV of free energy are stored in the form of redox equivalent photoproducts. Recombination requires tens of milliseconds in fluid solution and tens of microseconds in the thin films. The recombination follows the expected second-order equal concentration kinetics; however, uncertainties in the appropriate path length make it difficult to quantify the true second-order rate constant within the mesoporous films.[9]

The transient spectroscopic data also demonstrate that the reduced sensitizers do not inject electrons into TiO_2 under these conditions, step 2 in eq 2. The first reduction of the Ru(II) compounds studied is localized on the bpz (or dpp) ligand and

is not metal-based, i.e., $Ru^{II}(deeb)_2(bpz^-)^+$. Therefore, electron injection would be a remote process occurring from a ligand that is not directly bonded to the semiconductor surface. Rapid subnanosecond electron transfer from excited states localized on ligands remote to the semiconductor surface have been previously demonstrated.[23] Since the reduced Ru compounds have long microsecond lifetimes, the lack of injection is not likely to be kinetic in origin and indicates that the conduction band edge is not energetically accessible, i.e., $E_{cb} < -1.0$ V vs SCE.

The quenching rate constants, k_q, measured for eq 10 may not correspond to the true electron-transfer rate constants and must be corrected for possible contributions from diffusion.[24] A kinetic mechanism that incorporates a diffusional preequilibrium step is shown below, eqs 11 and 12.

$$Ru(deeb)_2(bpz)^{2+}* + PTZ \underset{k_{-diff}}{\overset{k_{diff}}{\rightleftharpoons}} [Ru(deeb)_2(bpz)^{2+}*, PTZ] \quad (11)$$

$$[Ru(deeb)_2(bpz)^{2+}*, PTZ] \xrightarrow{k_{et}} [Ru(deeb)_2(bpz^-)^+, PTZ^+] \quad (12)$$

A steady-state approximation yields eq 13 where $K_a = k_{diff}/k_{-diff}$.

$$\frac{1}{k_q} = \frac{1}{k_{diff}} + \frac{1}{k_{et}K_a} \quad (13)$$

When the time scales for diffusion and electron transfer are comparable, the observed quenching rate constant has contributions from both. In the limit that $k_{diff} \ll k_{et}K_a$, the reaction is diffusion controlled. In the other limit, electron transfer is slow compared to diffusion and k_q is equal to the product of K_a and k_{et}. The diffusion-controlled rate constant in acetonitrile at 25 °C can be calculated from the Debye−Smoluchowski−Stokes−Einstein relations. For $Ru(bpy)_3^{2+}$ with neutral organic donors it has been calculated to be $k_{diff} = 2.1 \times 10^{10}$ M^{-1} s^{-1}.[24] The quenching constants measured experimentally approach this limit and corrections for diffusion using eq 12 are therefore warranted, Table 3.

The electron-transfer rate constants are found to increase with driving force consistent with electron transfer in the Marcus normal region. The trend is clear both in fluid solution and in the mesoporous thin films. The rate constants measured in the latter media are consistently a factor of 2 to 3 slower. Since diffusion of the Ru(II) compounds is inhibited by carboxylate binding to the metal oxide surface, quenching likely originates mainly from PTZ diffusion. The quenching rate constant is therefore lower, as has been previously found at aqueous colloidal interfaces.[25] If we assume that the electron-transfer rate constants would be within experimental error the same, then $k_{diff} \sim 3 \times 10^9$ M^{-1} s^{-1} within the mesoporous films. Sluggish electron transfer may also reflect small changes in the thermodynamics for electron transfer at the interface. In any case, it is possible to quench > 99% of the excited states with high PTZ concentrations, indicating that PTZ can access essentially all the surface-bound excited states within the nanostructured thin film.

The yield of electron transfer products in the mesoporous films is clearly much lower than that observed in fluid solution. It is experimentally difficult to quantify precise cage escape yields in these materials. However a crude estimate based on data like that shown in Figure 5 indicates that the yield is at least 2/3 lower than that in solution. Cage escape yields following reductive electron transfer are known to be high in fluid solution and this implies a cage escape yield <0.3 on the nanocrystalline TiO_2 surface.[26] The low yield of charge-separated products is unfortunate from an energy conversion perspective and new strategies must be employed to increase the quantum yields. Previous workers have found that ionic strength and pH can be used to tune the cage escape yields at colloidal SiO_2 interfaces.[25] A negatively charged particle surface increases the cage escape yield when one of the charge-separated products is also negatively charged. Electrostatics of this nature appears to be relevant here as well. The TiO_2 is negatively charged and the oxidized phenothiazine product is positively charged. Therefore, following electron transfer, electrostatic interactions disfavor cage escape.

SCHEME 2

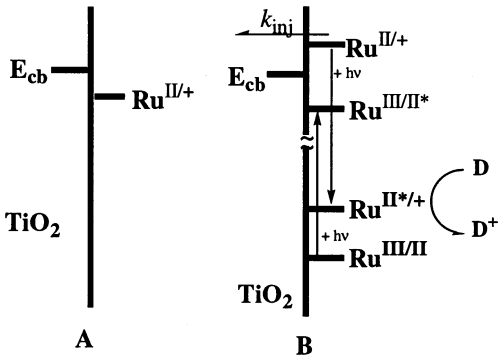

The rapid recombination of the PTZ^+ with the oxidized sensitizer in the TiO_2 film serves as direct evidence for electrostatic PTZ^+ surface adsorption. For diffusion-limited charge recombination in acetonitrile at these concentrations, there is no measurable loss of PTZ^+ on a sub-microsecond time scale. In contrast, within the mesoporous TiO_2 films, almost half of the pairs recombine in the first microsecond. This may simply reflect the high local concentration within the meosporous thin films, but is highly suggestive of recombination to PTZ^+ absorbed on the semiconductor surface. Using pH, or specific cation adsorption, to increase the cage escape yield would also shift the energetic position of E_{cb} and could change the sensitization mechanism. It would eliminate many of the possible benefits of having the reduced sensitizer inject the electron rather than the excited state. This point is elaborated upon further below.

Implications for Photogalvanic Cells. Photogalvanic cells were the hallmark molecular solar cells of the 1940s to 1960s.[27] In general, these cells operated by photoinduced charge separation in fluid solution followed by diffusion of the separated charges to dark electrodes. The efficiency of such cells was generally very low, < 1% in part due to competitive light absorption and difficulties with collecting the separated charges. Many of the obstacles have been overcome by the Grätzel approach.[2] The mesoporous nanocrystalline thin films provide a high surface area for sensitizer attachment, and hence efficient light harvesting, that requires only one of the separated charges to diffuse. To our knowledge, this report represents the first attempt to prepare dye-sensitized photogalvanic regenerative solar cells with these same materials. In terms of practical applications, the attempt failed. The reduced sensitizers did not inject electrons into the semiconductor, so the solar energy conversion was disappointingly low. This occurs because the conduction band is not energetically accessible, $E_{cb} < E°(Ru^{II/+})$, Scheme 2A. Nevertheless, some insights into how efficient

SCHEME 3

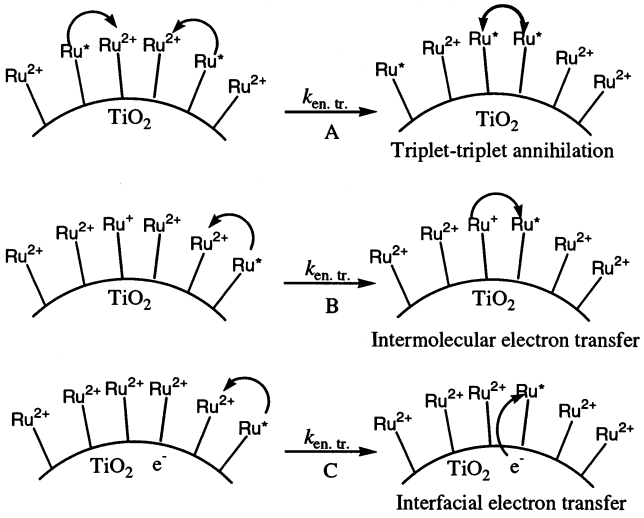

photogalvanic solar cells might be prepared in the future and some possible advantages of this approach are discussed below.

A potential advantage of having the reduced Ru(II) state inject an electron into the semiconductor rather than the excited state, is that the former is a stronger reductant. For the sensitizers under study, the energy difference is 300 to 400 mV and this is typical of Ru(II) sensitizers.[19] This means that Ru(II) sensitizers that are weak excited-state reductants may not sensitize TiO_2 under conditions where the reduced sensitizer could, Scheme 2B. Sensitizers with low-lying π^* orbitals that efficiently absorb light in the red and near-infrared region may therefore yield higher photocurrent efficiencies when the reduced sensitizer injects the electron.[28]

Reduced sensitizer injection may also improve the open circuit photovoltages of regenerative dye-sensitized solar cells. In the state-of-the-art cells, incident photons are converted to electrons in an external circuit near-quantitatively.[2] However, less than 1/2 of the free energy stored in the sensitizer excited state is converted to Gibbs free energy in the molecular solar cell.[2] Therefore, the sensitization kinetics are well optimized while the thermodynamics are not. In their original *Natur*e paper, Grätzel and O'Regan reported that the open circuit photovoltage was increased, and the photocurrent decreased, when the cation in the electrolyte was changed from Li^+ to tetrabutylammonium.[5] Studies since have shown that Li^+ adsorption to the TiO_2 surface shifts the conduction band positive promoting excited-state electron injection at the cost of lowering the quasi-Fermi level of the TiO_2.[29,30] If the injection yield could be kept high without introducing Li^+, then the power conversion efficiency would increase. In principle, the reduced sensitizer could accomplish this.

A key difference between the two sensitization mechanisms is the state that undergoes diffusional quenching, the excited state versus the oxidized state. In the latter case, the excited sensitizer can be very short-lived and indeed this has been found to be the case.[31] Long-lived excited states are needed for diffusional quenching and when sensitizers are arranged in close proximity, new energy-wasting pathways are introduced. One such pathway was already mentioned above, excited-state−excited-state annihilation reactions that are rate limited by intermolecular energy transfer across the semiconductor surface, Scheme 3A. The number of intermolecular Ru* → Ru "hops" that an excited state can undergo is unknown in the present system. However, recent Monte Carlo simulations for Ru(II) complexes weakly coupled through a polymer backbone reveal a Ru* → Ru hopping rate of 1−4 ns, and suggest that an excited state with a microsecond lifetime in a close-packed monolayer could undergo a thousand hops.[32] This would indicate that the sensitizer excited states under study can migrate across the *entire* nanoparticle surface within its lifetime.

Facile energy transfer allows translation of the excited state to encounter other excited states, impurities, or other species that could quench it, Scheme 3. For example, excited-state reduction by a reduced ruthenium compound would be energetically favored (by over 2 eV for the compounds under study), Scheme 3B. In cases where the reduced sensitizers inject electrons, the TiO_2 electron could also reduce the MLCT excited state.[33]

Collectively, the electron-transfer quenching pathways in Scheme 3B and C could lead to a type of "super quenching" where multiple excited states are deactivated by a single quencher.[34] For these processes to be significant, the rate constant for photoreduction would have to be competitive with intermolecular energy transfer away from the quenching site. No experimental evidence for these processes was obtained and the decreased rate constants measured for the mesoporous films relative to solution suggest that this is not a significant excited-state decay pathway, presumably because of the low yield of charge-separated products. Nevertheless, this reaction could be a significant obstacle for the preparation of efficient photogalvanic dye-sensitized cells. One method for avoiding these deleterious processes is to eliminate diffusion by covalently binding an electron donor directly to the sensitizer.[35]

Conclusion

The products of reductive electron-transfer reactions at sensitized semiconductor interfaces have been studied for the first time. There is strong experimental evidence that the reduced ruthenium compounds, like the excited states, do not inject electrons into TiO_2. This indicates that the acceptor states in TiO_2, presumably the conduction band, are more negative on an electrochemical scale than −1.0 V vs SCE under these conditions. In principle, it may be possible to shift the conduction band edge with pH, cations, or by utilizing alternative semiconductor materials such that the reduced compounds are energetically capable of interfacial electron transfer.

The possibility of making efficient photogalvanic cells based on dye-sensitized nanocrystalline films appears to be very real, even though it was not realized here. It may be possible to significantly enhance both the spectral sensitivity and the open circuit photovoltages over what has been previously reported.[2] Rapid intermolecular energy transfer across the nanocrystalline semiconductor surface leads to triplet−triplet annihilation reactions that can lower the power conversion efficiency. In addition, excited-state energy migration may lead to additional excited-state deactivation pathways and a high sensitivity to impurities. The use of molecular sensitizers that undergo intramolecular electron transfer prior to interfacial electron transfer will eliminate excited-state diffusion and should enhance energy conversion efficiencies.

Acknowledgment. We thank the National Science Foundation for research support.

Supporting Information Available: Typical data for for $Ru(deeb)(bpz)_2^{2+}$ and $Ru(deeb)_2(dpp)^{2+}$. This material is available free of charge via the Internet at http://pubs.acs.org.

References and Notes

(1) Gerischer, H. *Photochem. Photobiol.* **1972**, *16*, 243−260.
(2) Grätzel, M. *Nature* **2001**, *414*, 338−344.

(3) Qu, P.; Meyer, G. J. Dye-Sensitized Electrodes. In *Electron Transfer in Chemistry*; Balzani, V., Ed.; 2000; Part 2, Vol. IV, Chapter 2, pp 355−411.

(4) (a) Kirsch and co-workers have correlated Stern−Volmer constants calculated from luminescence and photocurrent measurements at planar electrodes: Ortmans, I.; Moucheron, C.; Kirsch-De Mesmaker, A. *Coord. Chem. Rev.* **1998**, *168*, 233−271. (b) In many other cases, it was not possible to identify the sensitization mechanism, see for example: Fox, M. A.; Nobs, F. J.; Voynick, T. A. *J. Am. Chem. Soc.* **1980**, *102*, 4036−4039.

(5) O'Regan, B.; Grätzel, M. *Nature* **1991**, *353*, 737−739.

(6) (a) Tachibana, Y.; Moser, J. E.; Grätzel, M.; Klug, D. R.; Durrant, J. *J. Phys. Chem.* **1996**, *100*, 20056−20062. (b) Hannappel, T.; Burfeindt, B.; Storck, W.; Willig, F. *J. Phys. Chem. B* **1997**, *101*, 6799−6807. (c) Heimer, T. A.; Heilweil, E. J. *J. Phys. Chem. B* **1997**, *101*, 10990−10996. (d) Benko, G.; Kallioinen, J. E.; Korppi-Tommola, J. E. I.; Yartsev, A. P.; Sundstrom, V. *J. Am. Chem. Soc.* **2002**, *124*, 489−494.

(7) Nasr, C.; Hotchandani, S.; Kamat, P. V. *J. Phys. Chem. B* **1998**, *102*, 4944−4951.

(8) Thompson, D. W.; Kelly, C. A.; Farzad, F.; Meyer, G. J. *Langmuir* **1999**, *15*, 650−653.

(9) Argazzi, R.; Bignozzi, C. A.; Heimer, T. A.; Castellano, F. N.; Meyer, G. J. *J. Phys. Chem. B* **1997**, *101*, 2591−2597.

(10) Alternative redox mediators for dye-sensitized solar cells represent an active area of research. See for example: (a) Oskam, G.; Bergeron, B. V.; Meyer, G. J.; Searson, P. C. *J. Phys. Chem. B* **2001**, *105*, 6867−6873. (b) Busbammer, H.; Moser, J. E.; Zakeeruddin, S. M.; Nazeeruddin, M. K.; Grätzel, M. *J. Phys. Chem. B* **2001**, *105*, 10461−10464.

(11) Crutchley, R. J.; Lever, A. B. P. *Inorg. Chem.* **1982**, *21*, 2276−2282.

(12) Evans, I. P.; Spencer, A.; Wilkinson, G. *J. C. S. Dalton* **1973**, 204−209.

(13) (a) Heimer, T. A.; D'Arcangelis, S. T.; Farzad, F.; Stipkala, J. M.; Meyer, G. J. *Inorg. Chem.* **1996**, *35*, 5319−5324. (b) Galoppini, E.; Guo, W.; Zhang, W.; Hoertz, P. G.; Qu, P.; Meyer, G. J. *J. Am. Chem. Soc.* **2002**, *124*, 7801−7811.

(14) Castellano, F. N.; Heimer, T. A.; Thandasetti, M.; Meyer, G. J. C*hem. Mater.* **1994**, *6*, 1041−1048.

(15) (a) Arnold, D. R.; Baird, N. C.; Bolton, J. R.; Brand, J. C. D.; Jacobs, P. W. M.; DeMayo, P.; Ware, W. R. *Photochemistry. An Introduction*; Academic Press: New York and London, 1974; p 13. (b) Rehm, D.; Weller, A. *Isr. J. Chem.* **1970**, *8*, 259−267.

(16) Kelly, C. A.; Thompson, D. W.; Farzad, F.; Meyer, G. J. *Langmuir* **1999**, *15*, 731−737.

(17) Lakowicz, J. R. *Principles of Fluorescence Spectroscopy*, 2nd ed.; Plenum Press: New York, 1999.

(18) Bergeron, B. V. Unpublished results.

(19) (a) Crutchley, R. J.; Lever, A. B. P. *J. Am. Chem. Soc.* **1980**, *102*, 7128−7130. (b) Prasad, D. R.; Hessler, D.; Hoffman, M. Z.; Serpone, N. *Chem. Phys. Lett.* **1985**, *121*, 61−64. (c) Rillema, D. P.; Allen, G.; Meyer, T. J.; Conrad, D. *Inorg. Chem.* **1983**, *22*, 1617−1622.

(20) Kalyanasundaram, K. *Photochemistry of Polypyridine and Porphyrin Complexes*; Academic Press: London, 1992.

(21) (a) Farzad, F.; Thompson, D. W.; Kelly, C. A.; Meyer, G. J. *J. Am. Chem. Soc.* **1999**, *121*, 5577−5578. (b) Trammell, S. A.; Yang, J.; Sykora, M.; Fleming, C. N.; Odobel, F.; Meyer, T. J. *J. Phys. Chem. B* **2001**, *105*, 8895−8904.

(22) (a) Milosavijevic, B. H.; Thomas, J. K. *J. Phys. Chem.* **1983**, *87*, 616−621. (b) Kennelly, T.; Gafney, H. D.; Braun, M. *J. Am. Chem. Soc.* **1985**, *107*, 4431−4440. (c) Fan, J.; Shi, W.; Strekas, T. C.; Gafney, H. D. *J. Phys. Chem.* **1989**, *93*, 373−376.

(23) (a) Argazzi, R.; Bignozzi, C. A.; Heimer, T. A.; Meyer, G. J. *Inorg. Chem.* **1997**, *36*, 2−3. (b) Qu, P.; Thompson, D. W.; Meyer, G. J. *Langmuir* **2000**, *16*, 4662−4671.

(24) Meyer, T. J. *Prog. Inorg. Chem.* **1982**, *30*, 389−439.

(25) (a) Willner, I.; Yang, J.-M.; Laane, C.; Otvos, J. W.; Calvin, M. *J. Phys. Chem.* **1981**, *85*, 3277−3282. (b) Degani, Y.; Willner, I. *J. Am. Chem. Soc.* **1983**, *105*, 6228−6233.

(26) Mallouk, T. E.; Krueger, J. S.; Mayer, J. E.; Dymond, C. M. G. *Inorg. Chem.* **1989**, *28*, 3507−3510.

(27) Albery, W. J. *Acc. Chem. Res.* **1982**, *15*, 142−149.

(28) (a) Argazzi, R.; Bignozzi, C. A.; Heimer, T. A.; Castellano, F. N.; Meyer, G. J. *Inorg. Chem.* **1994**, *33*, 5741−5749. (b) Nazeeruddin, Md. K.; Pechy, P.; Renouard, T.; Zakeeruddin, S. M.; Humphry-Baker, R.; Comte, P.; Liska, P.; Cevey, L.; Costa, E.; Shklover, V.; Spiccia, L.; Deacon, G. B.; Bignozzi, C. A.; Gratzel, M. *J. Am. Chem. Soc.* **2001**, *123*, 1613−1620.

(29) (a) Kelly, C. A.; Thompson, D. W.; Farzad, F.; Stipkala, J. M.; Meyer, G. J. *Langmuir* **1999**, *15*, 7047−7054. (b) Qu, P.; Meyer, G. J. *Langmuir* **2001**, *17*, 6720−6728.

(30) (a) Redmond, G.; Fitzmaurice, D. *J. Phys. Chem.* **1993**, *97*, 1426−1430. (b) Enright, B.; Redmond, G.; Fitzmaurice, D. *J. Phys. Chem.* **1994**, *98* (8), 6195−6200.

(31) (a) Ferrere, S.; Gregg, B. A. *J. Am. Chem. Soc.* **1998**, *120*, 843−844. (b) Islam, A.; Hara, K.; Singh, L. P.; Katoh, R.; Yanagida, M.; Murata, S.; Takahashi, Y.; Sugihara, H.; Arakawa, H. *Chem. Lett.* **2000**, 490−494.

(32) Fleming, C. N.; Maxwell, K. A.; DeSimone, J. M.; Meyer, T. J.; Papanikolas, J. M. *J. Am. Chem. Soc.* **2001**, *123*, 10336−10347.

(33) Long-lived excited states have been observed on reduced TiO_2 under conditions where reductive quenching like that shown in Scheme 3C would be expected. (a) O'Regan, B.; Moser, J. E.; Anderson, M.; Grätzel, M. *J. Phys. Chem.* **1990**, *94*, 8720−8726. (b) Kamat, P. V.; Bedja, I.; Hotchandi, S.; Patterson, L. K. *J. Phys. Chem.* **1996**, *100*, 4900−4905. (c) Heimer, T. A.; Meyer, G. J. *J. Lumin.* **1996**, *70*, 468−478. (d) Lemon, B. I.; Hupp, J. T. *J. Phys. Chem. B* **1999**, *103*, 3797−3799.

(34) (a) Swager, T. M. *Acc. Chem. Res.* **1998**, *31*, 201−207. (b) Chen, L.; McBranch, D. W.; Wang, H.-L.; Helgeson, R.; Wudl, F.; Whitten, D. G. *Proc. Natl. Acad. Sci. U.S.A.* **1999**, *96*, 12287−12292. (c) Harrison, B. S.; Ramey, M. B.; Reynolds, J. R.; Schanze, K. S. *J. Am. Chem. Soc.* **2000**, *122*, 8561−8562.

(35) (a) Argazzi, R.; Bignozzi, C. A.; Heimer, T. A.; Castellano, F. N.; Meyer, G. J. *J. Am. Chem. Soc.* **1995**, *117*, 11815−11816. (b) Bonhote, P.; Moser, J.-E.; Humphry-Baker, R.; Vlachopoulos, N.; Zakeeruddin, S. M.; Walder, L.; Gratzel, M. *J. Am. Chem. Soc.* **1999**, *121*, 1324−1331. (c) Kleverlaan, C. J.; Alebbi, M.; Argazzi, R.; Bignozzi, C. A.; Hasselmann, G. M.; Meyer, G. J. *Inorg. Chem.* **2000**, *39*, 1342−1343.